ELSEVIER

Thermochimica Acta 377 (2001) 51–61

thermochimica acta

www.elsevier.com/locate/tca

Equilibrium, nonequilibrium, and nonlinear enthalpy relaxation in a supercooled ionic liquid $[Ca(NO_3)_2]_{0.4}(KNO_3)_{0.6}$

I.K. Moon, Y.H. Jeong*

Department of Physics and electron Spin Science Center, Pohang University of Science and Technology, Pohang, Kyungbuk 790-784, South Korea

Received 9 October 2000; received in revised form 23 March 2001; accepted 26 March 2001

Abstract

We investigated extensively equilibrium, nonequilibrium, and nonlinear aspects of the enthalpy relaxation in a supercooled liquid $[Ca(NO_3)_2]_{0.4}(KNO_3)_{0.6}$. The equilibrium properties of relaxation, which are described in the framework of linear response theory, were determined from the frequency-dependent heat capacity measurements. The nonequilibrium and nonlinear aspects of relaxation were investigated by differential scanning calorimetry and time-domain dynamic calorimetry. It was found that the nonequilibrium relaxation can be fully accounted for in terms of the equilibrium one if the latter is properly extended, and that the successful extension of the equilibrium linear relaxation function must include both nonstationariness and thermorheological complexity. No evidence of genuine nonlinear enthalpy response, aside from the nonequilibrium effects, was seen in the time-domain dynamic calorimetric data, even when a temperature jump as large as 8 K was imposed.

PACS: 64.70.P; 66.10.C

Keywords: Glass transition; Dynamic heat capacity; Enthalpy relaxation; Nonlinear relaxation

1. Introduction

The glass transition is considered as a dynamic phenomenon, of which transition temperature is determined by the experimental time scale, such as a cooling rate in differential scanning calorimetry (DSC) experiments. The structural relaxation time τ becomes longer than the experimental time scale below the glass transition temperature T_g, and the structure of a glassy state relaxes toward a more stable state, even though it is too slow to observe any appreciable change on the normal experimental time scale. Thus, a glass is thermodynamically unstable and in nonequilibrium, while a supercooled liquid above T_g can be regarded as a stable state in equilibrium[1] as far as there is no route to crystallization [1]. The glass transition, therefore, describes a process in which a system falls out of equilibrium and offers an opportunity to study the relationship between the fluctuations of an observable, enthalpy for instance, in equilibrium and its relaxation under nonequilibrium conditions (falling out of or recovering equilibrium). It is worthwhile to note that the glass transition is a

* Corresponding author. Tel.: +82-562-279-2078; fax: +82-562-279-8056.
E-mail address: yhj@postech.ac.kr (Y.H. Jeong).

[1] In this paper we use the term 'equilibrium' to refer to the supercooled liquid as is usual in the glass literature.

0040-6031/01/$ – see front matter
PII: S0040-6031(01)00541-X

typical example of ergodicity-breaking phenomena due to the elongation of the time scale of underlying dynamics. Since statistical mechanics rests on the ergodic principle, the glass transition constitutes a problem of fundamental interest.

Three aspects of the structural recovery, nonlinearity, asymmetry, and memory effects, are usually cited as characteristic features of the nonequilibrium relaxation in the glassy state [2–4]. There have been a number of efforts to adequately describe these features. To handle nonlinearity and asymmetry, Tool [2] proposed that the structural relaxation of a glassy state should be a function of not only temperature T, but also of another variable which can characterize the internal structure of the glass state. This variable was then called fictive temperature T_f, and was defined in such a way that the nonequilibrium value of a certain quantity at T is equal to the equilibrium value of the quantity at T_f [5].

Narayanaswamy [3] dealt with the memory effects by assuming that the structural recovery is governed by a single nonexponential relaxation function of a fixed shape and that the shift factor in its time scale is a function of T_f. These assumptions are referred to as the so-called thermorheological simplicity or time–temperature superposition. The time scale shift factor was later refined by Moynihan et al. [6,7] who introduced a nonlinearity parameter x ($0 \leq x \leq 1$) into an Arrhenius form as

$$\tau = \tau_0 \exp\left[\frac{x\Delta h^*}{RT} + \frac{(1-x)\Delta h^*}{RT_f}\right] \quad (1)$$

where τ_0 and Δh^* (energy barrier per mole) are constants and R is the ideal gas constant. They also took into account the nonstationary nature of nonequilibrium relaxation in interpreting their DSC results; following Narayanaswamy, they wrote the normalized relaxation function $\phi(t, t')$ as

$$\phi(t, t') = \exp\left[-\left(\int_{t'}^{t} \frac{dt''}{\tau}\right)^{\beta}\right]. \quad (2)$$

It is easily seen that Eq. (2) is a modification of the Kohlrausch–Williams–Watt (KWW) relaxation function, i.e. $\phi(t) = \exp[-(t/\tau)^{\beta}]$, under the assumption of thermorheological simplicity (i.e. β = constant).

However, it was pointed out that x has no clear physical interpretation and the Arrhenius temperature dependence of Eq. (1) in equilibrium (i.e. $T_f = T$) is in conflict with the well-known Vogel–Tammann–Fulcher (VTF) temperature dependence expressed by

$$\tau = \tau_0 \exp\left(\frac{D}{T - T_0}\right) \quad (3)$$

where D and T_0 are constants. Scherer [8] adopted the Adam–Gibbs (AG) theory [9] which explains the temperature dependence of τ in terms of the temperature variation of the size of cooperatively rearranging regions. Hodge [10,11] also used the AG theory in writing the temperature dependence of τ as

$$\tau = \tau_0 \exp\left[\frac{D}{T(1 - T_K/T_f)}\right] \quad (4)$$

where T_K is the Kauzmann temperature at which the configurational entropy goes to zero [12]. If the system is in equilibrium, then Eq. (4) recovers the VTF equation since T_0 is often found to be the same as T_K. From the analysis of the DSC data for various glass-forming materials using Eqs. (2) and (4), Hodge [11] showed a possibility that the glassy state nonequilibrium relaxation may be accounted for by proper extension of the equilibrium relaxation in the supercooled liquid state above T_g (recently Hutchinson suggested an alternative to the usual extension based on Eq. (4) [13,14]).

The recent progress of modulation calorimetry (or frequency-domain dynamic calorimetry) [15,16] enabled one to measure the equilibrium enthalpy relaxation associated with the glass transition in the wide dynamic range. It was shown in our previous paper [17,18] that the nonequilibrium enthalpy relaxation (the DSC results) in an ionic glass former, $[Ca(NO_3)_2]_{0.4}(KNO_3)_{0.6}$ (CKN), can be well described if the equilibrium enthalpy relaxation, directly obtained by frequency-domain dynamic calorimetry, is properly extended. The successful extension was accomplished by a model, based on the modified AG equation of Eq. (4), which takes into account the nonstationarity and thermorheological complexity of the relaxation function.

The present paper reports, in detail, on thorough and comprehensive investigations of nonequilibrium relaxation and nonlinear relaxation in CKN. Note that here we are making a distinction between nonequilibrium relaxation and nonlinear one (for definitions, see the next section). Nonequilibrium relaxation, of

course, can show nonlinear effects; however, it should be understood that the nonlinear effects due to the nonequilibrium nature of the system is physically different from genuine nonlinear relaxation as was already pointed out in [17]. We clearly demonstrate that there is no nonlinear relaxation in the glass transition and nonlinear effects in relaxation, if any, stem from the nonequilibrium nature of a given experiment. We also rigorously test if it is ever possible for one to do without thermorheological complexity in nonequilibrium relaxation, and check a model for nonequilibrium relaxation proposed by Ngai et al. [19].

2. Theoretical framework for enthalpy relaxations

In this section we set up a theoretical framework for the description of various enthalpy relaxations reported in this paper. Consider the general equation for the response $\varepsilon(t)$ of a system to an external perturbation $\sigma(t)$: [17]

$$\varepsilon(t) = \int_{-\infty}^{t} K_1(t,t')\sigma(t')\,\mathrm{d}t' + \int_{-\infty}^{t}\int_{-\infty}^{t} K_2(t,t',t'')\sigma(t')\sigma(t'')\,\mathrm{d}t'\,\mathrm{d}t'' + \cdots, \tag{5}$$

where ε is any strain quantity, σ an externally applied stress quantity, and K_1 and K_2 represent the response functions. K_1, of course, is the linear response function obtainable from linear response theory (LRT) [20], and K_2 and higher order terms depict nonlinear responses of the system (For more detailed derivation with full mathematical complexity, one may refer to [21].) From the statistical mechanical point of view, all the equilibrium or near-equilibrium properties of the system are described as a function of $\mathscr{H}_0/k_\mathrm{B}T$, where $\mathscr{H}_0$, k_B, and T are the Hamiltonian of the system, the Boltzmann constant, and the temperature, respectively. For the temperature variation δT, the perturbing term in the Hamiltonian can be obtained from $\mathscr{H}_0/k_\mathrm{B}(T+\delta T) \approx \mathscr{H}_0(1-\delta T/T)/k_\mathrm{B}T$. Thus, the external perturbing field σ in our case is represented by $\delta T/T$ which couples to the Hamiltonian of the system.

Both for modulation calorimetric measurements where we keep δT intentionally small and for nonequilibrium experiments where constant cooling or heating can be considered as a succession of small temperature jumps, $\delta T/T$ appears to be small if we consider the fact that the glass temperature is on the order of a few hundred degrees for most materials. Thus, only the first term in Eq. (5) needs to be considered for most equilibrium and nonequilibrium measurements. However, it is conceivable that one may be able to find nonlinear relaxations due to higher order terms in situations where δT is sufficiently large. In fact, the exploration of this nonlinear relaxation in the glass transition region of CKN was one of the purposes of the present investigation. We will come back to this point later, and now we continue with the linear response term.

For the isobaric thermal responses ε is equal to the enthalpy deviation from the equilibirum value, δH, per unit volume and Eq. (5) can be written as

$$\frac{\delta H(t)}{V} = \int_{-\infty}^{t} K_\mathrm{H}(t,t')\delta T(t')\,\mathrm{d}t' + C_p^\infty \delta T(t) \tag{6}$$

where V denotes the volume. Here we have taken δT as the perturbation instead of $\delta T/T$ following the usual definition of the heat capacity. Note that the contribution from the fast degrees of freedom, such as phonons is explicitly separated and denoted as C_p^∞, and K_H is the response function due to the slow relaxation of the system. One can also represent Eq. (6) in terms of the relaxation function $R(t,t') = \int_{-\infty}^{t'} K_\mathrm{H}(t,t'')\,\mathrm{d}t''$. It is quite straightforward to show that Eq. (6) becomes

$$\frac{\delta H(t)}{V} = \Delta C_p \int_{-\infty}^{t} [1-\phi(t,t')]\delta\dot{T}(t')\,\mathrm{d}t' + C_p^\infty \delta T(t) \tag{7}$$

where the relaxation strength and the normalized relaxation function are given by $\Delta C_p \equiv R(t,t)$ and $\phi(t,t') \equiv R(t,t')/R(t,t)$, respectively. The dot, of course, stands for the derivative.

Although Eq. (7) appears to be linear, it may become mathematically nonlinear if the function $\phi(t,t')$ itself changes in time. This kind of nonlinear response occurs as a result of the loss of equilibrium and therefore loss of stationarity, for example, due to the slowing down of the system dynamics during

the course of scanning experiments. The class of relaxations, which are within the domain of linear response theroy from the physical point of view but nevertheless mathematically nonlinear, will be called nonequilibrium relaxations.

3. Equilibrium relaxation and dynamic heat capacity

Since the details of modulation calorimetry [16] and of the equilibrium relaxation measurements [17,18] were reported earlier, we briefly summarize the results. For the system in equilibrium, the relaxation function has the additional property of being stationary, i.e. $\phi(t,t') = \phi(t-t')$. Then, the dynamic heat capacity as a function of the angular frequency ω is given by

$$C_p(\omega) = C_p^0 + \mathrm{i}\omega\Delta C_p \int_0^\infty \phi(t)\mathrm{e}^{\mathrm{i}\omega t}\,\mathrm{d}t, \tag{8}$$

where $C_p^0 \equiv C_p^\infty + \Delta C_p$ denotes the static specific heat capacity. In line with the general susceptibility of linear response theory, the dynamic heat capacity is a complex quantity; the physical meaning of the imaginary part of $C_p(\omega)$ is interpreted as the entropy increase of the heat reservoir [16].

Fig. 1 shows the real (C_p') and imaginary (C_p'') parts of the dynamic specific heat capacity versus $\log f$. As is easily seen from the data, the dynamics of the system slows down with decreasing temperature and the shape of C_p'' is asymmetrical. These features are typical of many glass formers; since it has been found that the KWW function adequately describes the dynamics for them, the data at each temperature were fitted to Eq. (8) with the KWW function. To enhance the precision, we used the set of real and imaginary data simultaneously in fitting; it is noted that since C_p^0 does not vary with temperature, the fitting was done with three parameters, i.e., ΔC_p, τ, and β. The best-fit curves drawn through the data indicate that the KWW function is reasonable in describing the equilibrium enthalpy relaxation of CKN.

In Fig. 2(a), τ obtained from the fitting is shown against $1/T$. The data illustrate that τ is not behaving in an Arrhenius fashion, but in a VTF one. The solid

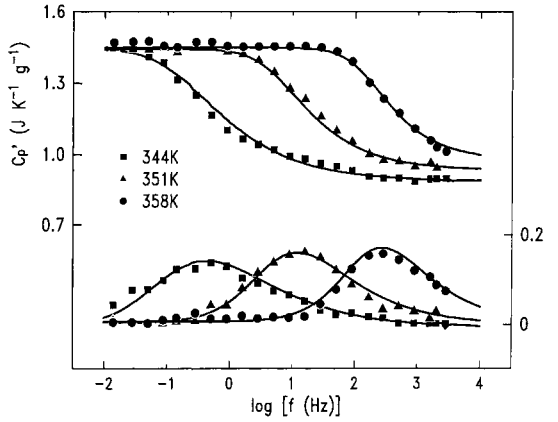

Fig. 1. Real (C_p') and imaginary (C_p'') parts of the dynamic specific heat capacity of $[Ca(NO_3)_2]_{0.4}(KNO_3)_{0.6}$ as a function of frequency. The solid lines are the fitting results with the KWW function: $\beta = 0.53$ (344 K), 0.57 (351 K), and 0.62 (358 K).

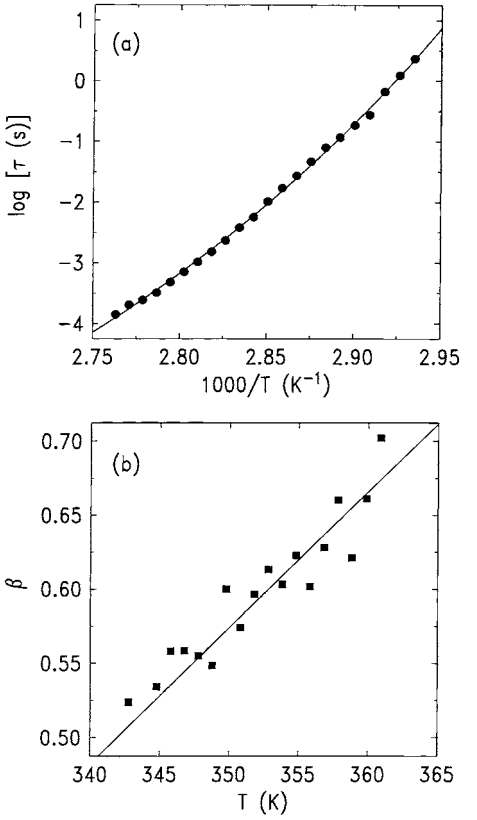

Fig. 2. (a) The temperature dependence of τ. The solid line denotes the best-fit result using the Vogel–Fulcher equation. (b) The temperature dependence of β. A linear function of T is used for fitting. The uncertainty in the value of β is within ± 0.02.

line represents the best fit to the data using the VTF form. The fitting procedure yielded the values for parameters: $\tau_0 = 10^{-14.6\pm1.1}$ s, $D = 1800 \pm 320$ K, $T_0 = 288 \pm 8$ K. Fig. 2(b) shows the exponent β versus T. From the figure, it is found that β varies linearly with T, which suggests the thermorheological complexity. The significance of this behavior is that any analysis based upon the assumption that $\beta =$ constant (i.e. thermorheological simplicity) may not be correct, especially in nonequilibrium situations. It is noted that the linear variation of β as a function of T, $\beta = \alpha(T - T_0)$ with $\alpha = 0.0092$, can be represented as $\beta = (T - T_0)/(T^* - T_0)$. This defines a hypothetical characteristic temperature T^*, whose significance is discussed in the final section.

4. Nonequilibrium relaxation and differential scanning calorimetry

In this section, we show that the nonequilibrium enthalpy relaxation associated with the glass transition of CKN is quantitatively accountable in terms of the equilibrium relaxation results presented in the previous section. While the modulation amplitude δT is kept intentionally small in modulation calorimetry to stay in the equilibrium regime, heat capacity is measured under nonstationary conditions induced by constant temperature-scanning rates in DSC experiments. However, the temperature scanning in DSC measurements is completely equivalent to a succession of small temperature steps, and therefore, if the nonstationariness is properly taken into account, Eq. (7) should also be valid in describing the nonequilibrium situations of DSC experiments.

The definition of T_f for enthalpy can be written by [6,7]

$$H(T) = H_l(T_f) - \int_T^{T_f} C_{pg}(T')\,dT', \tag{9}$$

where $H(T)$ is the measured enthalpy and $H_l(T)$ the enthalpy of the supercooled liquid in equilibrium. Since C_{pg} represents the contribution from the fast degrees of freedom, Eq. (9) states that the enthalpy due to the relaxing modes is characterized by T_f, while the temperature of the fast degree of freedom is T. Thus, T_f signifies the temperature of the structural configuration of the relaxing modes. It can also be shown easily that dT_f/dT is equal to the normalized heat capacity due to the relaxing components, i.e.

$$\frac{dT_f}{dT} = \frac{C_p(T) - C_{pg}(T)}{C_{pl}(T_f) - C_{pg}(T_f)}. \tag{10}$$

Then we may focus on calculating T_f and its temperature derivatives and compare them with the the experimental data.

In order to find an equation for T_f, one may remove the contribution due to the fast degrees of freedom from Eq. (7) and then take the normalization factor into account:

$$T_f(t) = T^{(0)} + \int_0^t [1 - \phi(t,t')]\delta\dot{T}(t')\,dt' \tag{11}$$

where $T^{(0)}$ is the initial temperature at which the system is in equilibrium. Note that even if Eq. (11) is in the form of linear response, the nonstationariness of $\phi(t,t')$ can cause nonlinear behaviors in the nonequilibrium relaxation. To evaluate Eq. (11), $\phi(t,t')$ may be specified as an extension of the equlibrium relaxation function if β is not a function of temperature:

$$\phi(t,t') = \phi(t-t') = \exp\left[-\left(\frac{t-t'}{\tau}\right)^{\beta}\right]. \tag{12}$$

For a constant cooling or heating rate q, then Eq. (11) is rewritten by

$$T_f(T) = T^{(0)} + \int_{T_0}^{T}\left\{1 - \exp\left[-\left(\int_{T'}^{T}\frac{dT''}{q\tau}\right)^{\beta}\right]\right\}dT', \tag{13}$$

which can be calculated using the following discrete form which represents the evolution of T_f after the nth temperature step $\Delta T^{(n)}$ [6,7]

$$T_f^{(n)} = T^{(0)} + \sum_{j=1}^{n}\left\{1 - \exp\left[-\left(\sum_{k=j}^{n}\frac{\Delta T^{(k)}}{q^{(k)}\tau^{(k)}}\right)^{\beta}\right]\right\}\Delta T^{(j)}, \tag{14}$$

where $\tau^{(k)}$ is determined by the modified AG equation as

$$\tau^{(k)} = \tau_0 \exp\left[\frac{D}{T^{(k)}(1 - T_0/T_f^{(k-1)})}\right], \tag{15}$$

and the initial condition is $T_f^{(0)} = T^{(0)}$.

However, difficulty arises if β varies as a function of temperature as in the case of CKN. Since it is impossible to calculate Eq. (14) numerically, we resort to a scheme that the KWW function is approximated by a sum of Debye functions with distribution of relaxation times (τ_{Di}) as [6,22]

$$\exp\left[-\left(\frac{t-t'}{\tau}\right)^{\beta}\right] \simeq \sum_{i=1}^{N} g_i \exp\left(-\frac{t-t'}{\tau_{Di}}\right), \qquad (16)$$

where g_i is the normalized weighting factor for τ_{Di}, which satisfies $\sum_{i=1}^{N} g_i = 1$. The distribution of the relaxation times can be represented either by the prefactor distribution with the barrier fixed by the configurational entropy at $\Delta/(1 - T_0/T_f)$ or by the distribution of the barrier itself around $\Delta/(1 - T_0/T_f)$. While the physical interpretation of the former representation is not easy compared to the latter, it gives the best results and so we used the former in the present calculation. In fact, one may raise the question about the physical basis for using the distribution of Debye relaxations. However, this would take us to the long-running debate, and here we are merely content with taking advantage of mathematical equivalence. Now that each Debye relaxation time τ_{Di} is time-dependent via T_f, each exponential relaxation function of Eq. (16) is replaced by $\exp[-\int_{t'}^{t} dt''/\tau_{Di}(t'')]$. Note that this is equivalent to assuming the exponential decay at each instant with τ_{Di} of that moment. The time-varying nature of β is taken into account by making the distribution function g_i time-dependent. We also assumed that $\beta = \alpha(T_f - T_0)$, because the distribution of the relaxation times should be determined by the variable determining the structural configuration, i.e. T_f.

Then, the distribution after the kth temperature step is determined by $\alpha(T_f^{(k-1)} - T_0)$ as the case of τ in Eq. (15) since β determines the shape of the distribution. Fig. 3 shows the distributions corresponding for different values of β. In the practical calculation, the temperature step ΔT was set to 0.05 K. For the approximation of Eq. (16), we used the algorithm of singular value decomposition [23] with the Debye relaxation times which are equally spaced in logarithmic scale by

$$\log_{10}\tau_{Di} = \log_{10}\tau_{D1} + \left(\frac{i-1}{N}\right)\log_{10}\left(\frac{\tau_{DN}}{\tau_{D1}}\right), \qquad (17)$$

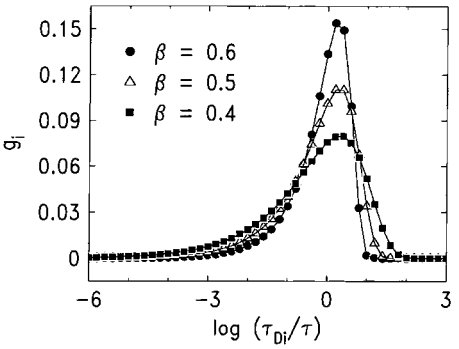

Fig. 3. The distribution of the Debye relaxation times for the KWW functions with different β values as designated in the figure.

where $\tau_{D1} = 10^{-10}\tau$, $\tau_{DN} = 10^{4}\tau$, $N = 71$. To improve the fitting precision, $4N$ data points of the KWW function between τ_{D1} and τ_{DN} were fitted.

The nonequilibrium relaxation in CKN was studied by measuring heat capacity at various scanning rates using a Perkin–Elmer DSC 7. Fig. 4 shows the DSC data measured at the labeled cooing rates and the heating rate of 10 K/min. The data on cooling show

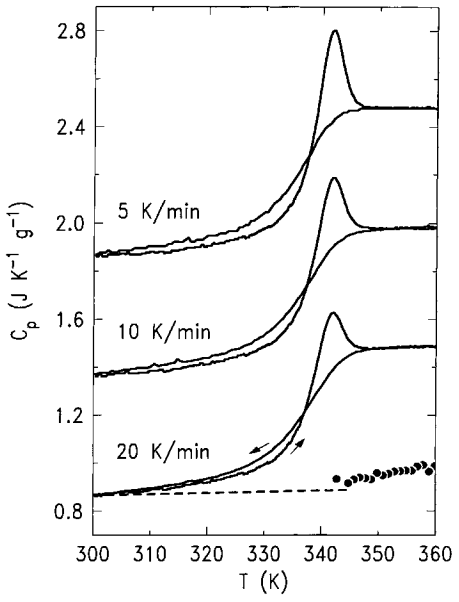

Fig. 4. DSC scanning results (solid lines) at labeled cooling and 10 K/min heating rates. The scale is correct for 20 K/min cooling data and others are displaced upwards for clarity. The arrows denote the scanning directions. The closed circles denote C_p^{∞} from the dynamic heat capacity data, while the broken line does C_{pg}.

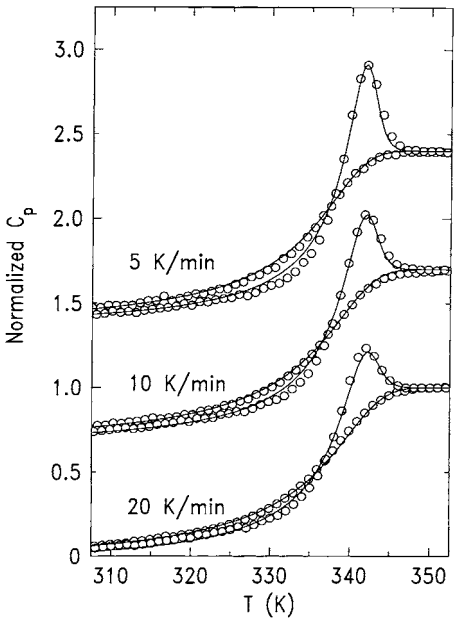

Fig. 5. The open circles represent the normalized heat capacity, $[C_p(T) - C_{pg}(T)]/[C_{pl}(T_f) - C_{pg}(T_f)]$, at labeled cooling and 10 K/min heating rates. The 5 and 10 K/min cooling data are displaced upwards. The solid lines from the calculation show excellent coincidence.

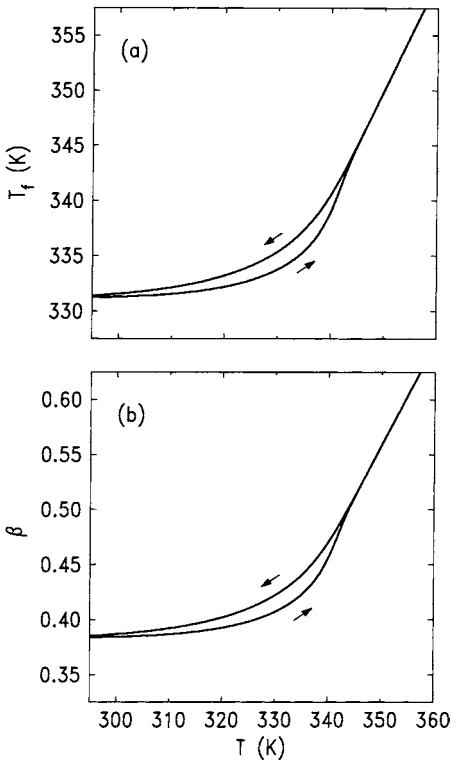

Fig. 6. T_f and β are shown as a function of temperature. These are the values which yield the best agreement between the experimental and theoretical data. (a) Calculated values of T_f for cooling and heating rates of 10 K/min. (b) Temperature dependence of β determined by $\alpha(T_f - T_0)$. The arrows represent the scanning directions.

a typical transition from the value of the liquid specific heat capacity (C_{pl}) at high temperature to the glass one (C_{pg}) at low temperature, while the data on heating are showing the peaks resulted by the system recovering equilibrium just above T_g.

Fig. 5 displays both the experimental and calculated data. Since the temperature derivative of T_f is equal to the normalized specific heat capacity as expressed in Eq. (10), the experimental C_p data were also normalized accordingly, that is, $[C_p(T) - C_{pg}(T)]/[C_{pl}(T_f) - C_{pg}(T_f)]$. One can see that the coincidence between the experimental and calculated data is striking and the main features of the temperature-scanning, cooling as well as heating, data were faithfully reproduced. Fig. 6(a) shows T_f, as a function of temperature, obtained from the calculation for the 10 K/min scanning rate. The hysteric temperature dependence of β, obtained from $\beta = \alpha(T_f - T_0)$, is shown in Fig. 6(b). It is stressed that β varies as a function of temperature, and does not remain constant.

The possibility of thermorheological simplicity, a long standing assumption in the literature, was investigated. If β is constant, T_f can be easily calculated without the approximation of Eq. (16). The results are shown in Fig. 7(a–c) for $\beta = 0.5$, 0.45, and 0.4, respectively. In Fig. 7(a) and (c), it is seen that the solid lines representing the calculated data deviate largely from the experimental data. It is even worse for the values of β greater than 0.5. For the calculated data with $\beta = 0.45$, the agreement between the experimental and calculated data seems reasonable as shown in Fig. 7(b). However, even in this case the statistical residual analysis indicates that the agreement is not as good as it is in Fig. 5. Furthermore, the value of $\beta = 0.45$ is completely unrelated to those obtained from the equilibrium measurements, and is nothing more than an ad hoc value. Thus, we conclude that the thermorheological simplicity is not a valid concept at least for one glass former, CKN.

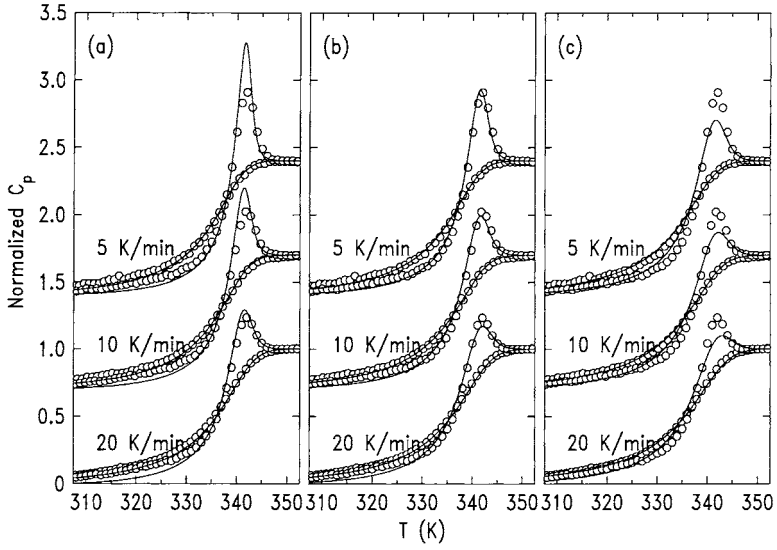

Fig. 7. The test of thermorheological simplicity. The solid lines represent the calculated data with temperature independent values of (a) $\beta = 0.5$, (b) 0.45, and (c) 0.4. In (a) and (c), the solid lines deviate largely from the experimental data. For the calculated data with β=0.45, the agreement between the experimental and calculated data seems reasonable (though not as good as in Fig. 5), but in this case the value of β is completely unrelated to that obtained from the equilibrium measurements.

Some years ago, a rather different type of the relaxation function for nonequilibrium situations was proposed by Ngai et al. [19] from their coupling theory. From the theory, they derive the following result for the relaxation function:

$$\frac{\mathrm{d}\ln\phi(t)}{\mathrm{d}t} = -\frac{\beta t^{\beta-1}}{\tau^{\beta}}. \tag{18}$$

If τ and β are time-independent as the case of the equilibrium relaxation, Eq. (18) gives the KWW function. In nonequilibrium condition, however, both τ and β may depend on time, so the relaxation function should be obtained by integrating Eq. (18). The integration yields

$$\phi(t) = \exp\left(-\int_0^t \frac{\beta t'^{\beta-1}}{\tau^{\beta}}\,\mathrm{d}t'\right). \tag{19}$$

However, it was pointed out by Hodge [24] that Eq. (19) depends on the time interval between the temperature steps used in calculation, which is obviously inconsistent with experimental observations. We tested this model using the previous calculation procedure. Both the experimental and calculated data are shown in Fig. 8 for the scanning rate of 10 K/min. It is seen that not only the calculated data

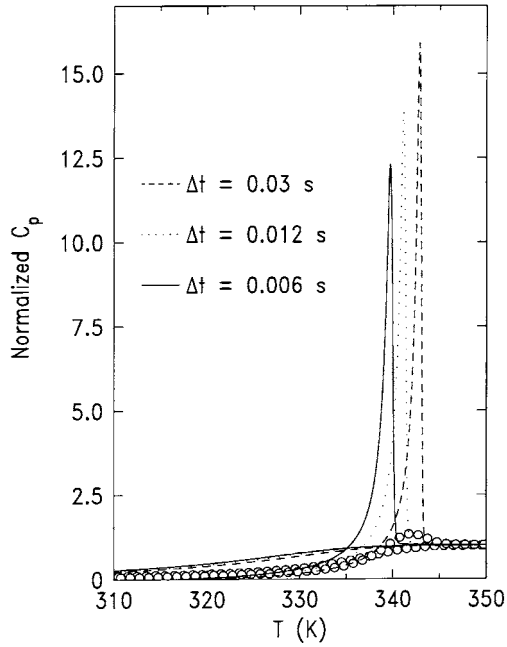

Fig. 8. The lines denote the calculation results using the model by Ngai et al. at 10 K/min scanning rate and labeled time steps. The open circles are the experimental data. Note that the calculation results vary wildly as different sizes for the time interval between temperature steps are used.

deviate largely from the experimental one, but also the calculation results show sensitive dependence on the time interval between temperature steps. Thus, it is concluded that not only the inability of Eq. (19) to fit the data implies its inadequateness in describing the nonequilibrium relaxation of CKN, but also the function itself contains inherent contradiction as the nonequilibrium relaxation function.

5. Nonlinear relaxation and time-domain dynamic calorimetry

In time-domain dynamic calorimetry, a certain amount of heat is applied instantaneously to a sample and its temperature response is examined in real time. Initially, applied heat is distributed only among phonon or fast degrees of freedom causing an instantaneous temperature jump, and then a portion of the energy slowly diffuses into the configurational (relaxing) degrees of freedom resulting in the decrease of the sample temperature. This temperature-relaxation experiment is the time-domain counterpart of modulation, or frequency-domain dynamic, calorimetry in the linear response regime. Time-domain dynamic calorimetry, however, has an additional feature which may be taken advantage of in studying nonlinear relaxation: while it is not easy to apply a large amount of power to a sample in modulation calorimetry, there is no difficulty in varying the temperature-jump size in the time-domain experiments. This unique feature of time-domain dynamic calorimetry allows one to study the nonlinear temperature relaxation induced by a large temperature-jump [16,25]. Since it is essential to maintain adiabaticity during the relaxation period after applying a heat in time-domain dynamic calorimetry, an adiabatic calorimeter was used for the investigation of nonlinear relaxation. The details of the experimental setup and operation of the adiabatic calorimeter were presented elsewhere [26].

In order to check if the time-domain calorimetric data can be understood within the same theoretical framework as the one used for the nonequilibrium measurements described in the previous section, we again calculated the temperature evolution according to Eq. (11) and compared with the experimental data. Only in this case, the adiabatic constraint was imposed in the calculation, and Eq. (10) becomes

$$-C_{pg}(T)\,\mathrm{d}T = [C_{pl}(T_f) - C_{pg}(T_f)]\mathrm{d}T_f, \tag{20}$$

and the instantaneous heat corresponds to $C_{pg}(T_i)\Delta T_j$ where T_i is the initial temperature in equilibrium and ΔT_j denotes the instantaneous temperature jump. The evolution of T after the nth time (calculation) step is given by

$$T^{(n)} = T^{(n-1)} - [C_{pl}(T_f^{(n)}) - C_{pg}(T_f^{(n)})](T_f^{(n)} - T_f^{(n-1)}), \tag{21}$$

where $T_f^{(n)}$ can be calculated using the initial conditions of $T^{(0)} = T_i + \Delta T_j$ and $T_f^{(0)} = T_i$.

In comparing the calculation results with the experimental data, it should be kept in mind that Eq. (21) is not valid in nonadiabatic situations which always prevail in the early times after applying heat instantaneously. As described in [26], an adiabatic calorimeter consists of multiple shields and is physically bulky, and therefore it takes time for the calorimeter to settle in the adiabatic condition. It turned out that the settling time for the adiabatic calorimeter used in the present measurements was about 1 min. It is then obvious that the relaxation time under investigation must be much longer than the settling time for time-domain dynamic calorimetry to yield meaningful results.

We carried out time-domain dynamic calorimetric measurements of supercooled CKN at 328 K where the relaxation time of the liquid is as long as several hundred minutes. Then the effect of the settling time should be negligible. The data points plotted in Fig. 9 represent the temperature relaxation of the sample following a temperature rise of $\Delta T_j = 1$ K. Also shown by the solid line in Fig. 9 is the theoretical results calculated as prescribed above. The nonadiabatic effect at early times, i.e., the effect of the settling time, was taken into account in calculation using the same method as in the temperature-scanning case of the previous DSC experiment (however, the early time data are not our concern). The arrow in the figure indicates the time at which the adiabaticity in the experiment is established and after which the adiabatic condition is maintained. It is seen that the coincidence between the experimental and calculated values is excellent for the data obtained under adiabaticity. This nearly perfect agreement vividly manifests the fact that the time-domain relaxation in supercooled CKN

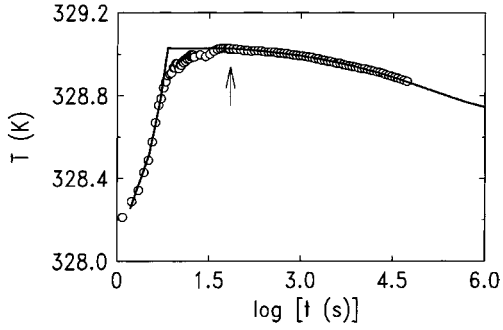

Fig. 9. The up-jump experiment in time-domain dynamic calorimetry. An initial temperature rise of 1 K is imposed on the system at $T_i = 328$ K by applying a precalculated amount of power to the sample, and the ensuing temperature variation is monitored. The adiabatic condition is achieved (arrow) after a transient period elapses, and then the temperature relaxes under the adiabatic condition. The circles represent the experimental data and the line is drawn from the calculated values, and they show excellent agreement. Notice the logarithmic scale in the time axis.

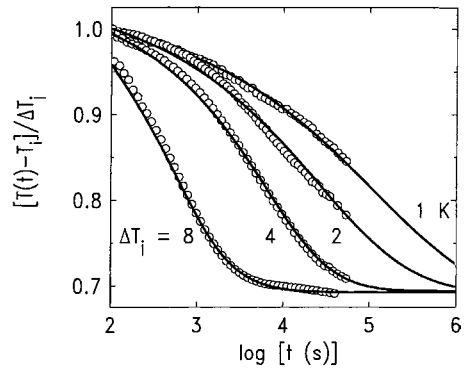

Fig. 10. The normalized temperature relaxation in up-jump experiments. Initially the system is at $T_i = 328$ K, and sudden temperature rises of magnitude $\Delta T_j = 1, 2, 4$, and 8 K are induced. After the transient period elapses, the temperature relaxation occurs under the adiabatic condition. From the normalized plot the nonlinear behavior is evident; however, this nonlinearity is fully accounted for in terms of the extended equilibrium relaxation function as indicated by solid lines.

following a temperature jump of modest size 1 K is purely of nonstationary, nonequilibirum nature.

In order to investigate the genuine nonlinear relaxation in supercooled CKN, we carefully examined the temperature relaxations caused by temperature jumps of various magnitudes. That is, an initial temperature rise of a certain magnitude ΔT_j was imposed on the system at $T_i = 328$ K by applying a precalculated amount of power to the sample, and the ensuing temperature variation was monitored. These measurements were repeated for $\Delta T_j = 1, 2, 4$, and 8 K. Strong nonlinearity is evident from the temperature relaxation plot normalized by the initial jump size ($\Delta T_j = 1, 2, 4$, and 8 K) as presented in Fig. 10 . However, this nonlinearity turns out to be accountable by allowing τ and β to vary in the course of relaxation (i.e. nonstationarity and thermorheological complexity) as is the case of the previous DSC results. The lines in Fig. 10 were again calculated from Eq. (21) and the excellent agreement persists not only for the data from small temperature jumps but also those from a large jump of 8 K. These results then suggest that the nonlinear terms in Eq. (5) does not play a role in the relaxation of supercooled CKN, which is also consistent with the recent investigation on the nonlinear thermal response at the glass transition of polymers using temperature modulated DSC [27]. We may add that we have not carried out down-jump experiments (as opposed to the present up-jump experiments) for technical reasons, but we expect that Eq. (21) would describe the down-jump experiments equally well.

6. Conclusions

We have extensively investigated equilibrium, nonequilibrium, and nonlinear aspects of the enthalpy relaxation in a representative glass former, supercooled $[Ca(NO_3)_2]_{0.4}(KNO_3)_{0.6}$. The equilibrium properties of relaxation were determined from the frequency-dependent heat capacity measurements, while the nonequilibrium aspects of relaxation were investigated by differential scanning calorimetry and time-domain dynamic calorimetry. It was found that the nonequilibrium relaxation can be fully accounted for in terms of the equilibrium one if the latter is properly extended, and that the successful extension of the equilibrium linear relaxation function must include both nonstationariness and thermorheological complexity.

Regarding the temperature dependence of β, i.e. thermorheological complexity, it was already noted that β may be expressed in the form of $\beta = (T - T_0)/(T^* - T_0)$, and this suggests a possible existence of another characteristic temperature T^* around 397 K. At T^* and above, the relaxation function would

become the Debye relaxation function with $\beta = 1$. This interpretation is in accordance with a recent molecular dynamics simulation, which predicts the same kind of nonexponential–exponential crossover accompanying non-Arrhenius to Arrhenius crossover in relaxation time at a temperature above T_g [28]. Since these crossovers originated from the variation of potential-energy barrier heights in the energy landscape of the system, it is of value to remind that Eq. (4) can be considered to be in the Arrhenius form with a temperature-dependent energy barrier height of $D/(1 - T_0/T)$ in equilibrium. Experimentally a more convincing evidence for an existence of the characteristic temperature T^* in supercooled liquids were found from the investigation of supercooled polypropylene glycol [29]. In polypropylene glycol it was seen that T^* (the temperature where β becomes 1) is indeed a temperature where the local Johari–Goldstein mode [30] merges with the cooperative main relaxation.

Despite its success, there is one caveat to be kept in mind in extending equilibrium relaxation into the nonequilibrium regime. Since we do not have a universally accepted theory for the equilibrium KWW function (not to mention the nonequilibrium case), we resorted to the idea of distribution of relaxation times and seeked to extend it. Our calculation yielded the best results when the distribution of the Debye relaxation times was assumed to be caused by the prefactor (τ_0) distribution with the energy barrier height fixed at $D/(1 - T_0/T_f)$. These procedures are really ad hoc without theoretical basis, and need to be justified by a physical theory.

No evidence of nonlinear enthalpy response, aside from the nonequilibrium effects, was seen in the time-domain dynamic calorimetry, even when a temperature jump as large as 8 K was imposed. This may be understandable, considering the fact that the temperature jump of $\delta T = 8$ K is equivalent to the perturbation of only $\delta T/T = 0.025$. Since it is technically difficult to impose a larger temperature jump than 8 K in calorimetric measurements, it may be worthwhile to attempt to find nonlinear behaviors in enthalpy relaxation with low T_g materials. Finally, it would be of value to carry out similar kind of extensive measurements for different class of materials to establish universality of the conclusions drawn from the present study.

Acknowledgements

This work was supported by the BK21 program initiated by the Korean Ministry of Education, the Pohang University of Science and Technology, and the POSCO company.

References

[1] M.D. Ediger, C.A. Angell, S.R. Nagel, J. Phys. Chem. 100 (1996) 13200.
[2] A.Q. Tool, J. Am. Ceram. Soc. 29 (1946) 240.
[3] O.S. Narayanaswamy, J. Am. Ceram. Soc. 54 (1971) 491.
[4] A.J. Kovacs, J.J. Aklonis, J.M. Huchinson, A.R. Ramos, J. Polym. Sci.: Polym. Phys. 17 (1979) 1097.
[5] A.Q. Tool, C.G. Eichlin, J. Am. Ceram. Soc. 14 (1931) 276.
[6] C.T. Moynihan et al., Ann. (NY) Acad. Sci. 279 (1976) 15.
[7] M.A. DeBolt, A.J. Easteal, P.B. Macedo, C.T. Moynihan, J. Am. Ceram. Soc. 59 (1976) 16.
[8] G.W. Scherer, J. Am. Ceram. Soc. 67 (1984) 504.
[9] G. Adam, J.H. Gibbs, J. Chem. Phys. 43 (1965) 139.
[10] I.M. Hodge, Macromolecules 19 (1986) 936.
[11] I.M. Hodge, Macromolecules 20 (1987) 2897.
[12] W. Kauzmann, Chem. Rev. 43 (1948) 219.
[13] S. Montserrat, P. Cortes, Y. Calventus, J.M. Hutchinson, J. Polym. Sci.: Polym. Phys. 38 (2000) 456.
[14] J.M. Hutchinson, S. Montserrat, Y. Calventus, P. Cortes, Macromolecules 33 (2000) 5252.
[15] N.O. Birge, S.R. Nagel, Phys. Rev. Lett. 54 (1985) 2674.
[16] Y.H. Jeong, Thermochim. Acta 304/305 (1997) 67.
[17] Y.H. Jeong, I.K. Moon, Phys. Rev. B 52 (1995) 6381.
[18] I.K. Moon, Y.H. Jeong, S.I. Kwon, Rev. Sci. Instrum. 67 (1996) 29.
[19] R.W. Rendell, K.L. Ngai, G.R. Fong, J.J. Aklonis, Macromolecules 20 (1987) 1070.
[20] R. Kubo, Rep. Prog. Phys. 29 (1966) 255.
[21] S. Lustig, R.M. Shay, J.M. Caruthers, J. Rheol. 40 (1996) 69.
[22] G.W. Scherer, J. Am. Ceram. Soc. 69 (1986) 374.
[23] W.H. Press et al., Numerical Recipes in C, Cambridge University Press, New York, 1992, pp. 650–655.
[24] I.M. Hodge, J. Non-Cryst. Solids 169 (1994) 211.
[25] H. Fujimori, Y. Adachi, M. Oguni, Phys. Rev. B 46 (1992) 14501.
[26] I.K. Moon, Y.H. Jeong, Rev. Sci. Instrum. 67 (1996) 3553.
[27] C. Schick, M. Merzlyakov, A. Hensel, J. Chem. Phys. 111 (1999) 2695.
[28] S. Sastry, P.G. Debenedetti, F.H. Stillinger, Nature 393 (1998) 554.
[29] I.K. Moon, Y.H. Jeong, T. Furukawa, Thermochim. Acta, in press.
[30] G.P. Johari, M. Goldstein, J. Chem. Phys. 53 (1970) 2372.